Simplified Lateral Torsional Buckling Equations
for I- and Channel-Section Members

by

Donald W. White
Professor
Structural Engineering, Mechanics and Materials

and

Se-Kwon Jung
Graduate Research Assistant

School of Civil and Environmental Engineering
Georgia Institute of Technology
Atlanta, GA 30332-0355
e-mail: dwhite@ce.gatech.edu
Phone: 404-894-5839
FAX: 404-894-0278

March 2003

Simplified Lateral Torsional Buckling Equations for I- and Channel-Section Members

DONALD W. WHITE and SE-KWON JUNG

Donald W. White is Professor, Structural Engineering, Mechanics and Materials, Georgia Institute of Technology, Atlanta, GA 30332-0355

Se-Kwon Jung is Graduate Research Assistant, Structural Engineering, Mechanics and Materials, Georgia Institute of Technology, Atlanta, GA 30332-0355

INTRODUCTION

A wide variety of exact and approximate forms of the fundamental beam-theory equations for lateral-torsional buckling (LTB) of open-walled section members have been employed within modern steel design standards (CSA 2001; AISC 1999 and 1989; AASHTO 1998; SAA 1998; SSRC 1998 and 1976; CEN 1993). The AISC (1999) LRFD Specification employs two parameters, denoted by X_1 and X_2, in its statement of the elastic LTB resistance for doubly-symmetric I-section members and channels. These parameters are a product of a particular algebraic arrangement of the exact equations, but their physical significance is somewhat difficult to understand. Hoadley (1991) shows that for rolled wide-flange shapes these terms can be approximated by simple functions of the flange thickness and section depth. However, his approximations do not apply to general built-up I-shapes and channels. The AISC (1989) Allowable Stress Design Specification employs a traditional double-formula approximation for the elastic LTB strength. The double-formula approach is obtained by neglecting the contributions from the St. Venant torsional rigidity GJ for deep narrow-flange sections, and by neglecting the contributions from the warping rigidity EC_w for stocky shallow sections with relatively wide flanges. Generally, the member strength is taken as the larger value obtained from these two simplifications. Several approximations are invoked in the development of these equations that also make them inappropriate for general built-up I-section members and channels. The AASHTO (1998) LRFD Specifications utilize another form of the exact doubly-symmetric open-walled section beam-theory equations, specialized to I-section members. Although the AASHTO equations are exact only for doubly-symmetric I-shapes, they are employed as an approximation for the elastic LTB strength of singly-symmetric noncomposite I-shapes with compact, noncompact or longitudinally-stiffened webs. Various other simplified expressions suggested in earlier developments can be found in (de Vries 1946), (Clarke and Hill 1960) and (SSRC 1976).

This paper presents a recommended simplified form of the fundamental beam-theory LTB equations for doubly-symmetric members, specialized to the elastic LTB resistance of I- and channel-section members. This recommended form is exact for doubly-symmetric I-section members and has the advantage of improved accuracy relative to the corresponding AASHTO (1998) equations when applied to singly-symmetric I-shapes, including composite I-section members in negative bending. Also, it avoids significantly conservative errors that occur within the double-formula approach for a wide range of rolled wide-flange shapes. Furthermore, the physical significance of each of the terms within the simplified equations is easy to understand. These equations are utilized as the base elastic LTB expressions within the AASHTO (2004) and AISC (2005) Specifications.

CONTEXT

The LTB provisions in AASHTO (1998 and 2004) and AISC (1999 and 2005) are based on the logic of identifying the two anchor points shown in Fig. 1 for the base case of uniform major-axis bending. Anchor point 1 is located at the length $L_b = L_p$ corresponding to development of the maximum potential flexural resistance under uniform major-axis bending (labeled as the compression flange stress F_{max} or the moment M_{max} in the figure). Anchor point 2 is located at the smallest length $L_b = L_r$ for which the LTB strength is governed by elastic buckling. The corresponding base moment and compression flange elastic stress levels are denoted in this paper by the symbols M_{yr} and F_{yr}, where $M_{yr} = F_{yr} S_{xc}$ and F_{yr} is the compression flange flexural stress corresponding to the nominal onset of yielding within the cross-section, including compression flange residual stress effects. The equivalent terms in AISC (1999) are represented by the symbols F_L and M_r. The term L_r is obtained generally as the length associated with elastic buckling at a compression flange major-axis bending stress of $F_{cr} = F_{yr}$. The anchor points in Fig. 1 subdivide the LTB problem into three regions, the "compact" or "plastic buckling" region, the "noncompact" or "inelastic buckling" region, and the "slender" or "elastic buckling" region. This is a powerful approach for quantifying the general LTB resistance in that it facilitates the handling of a number of complex issues. This approach is the framework for the discussion of the elastic LTB equations in this paper.
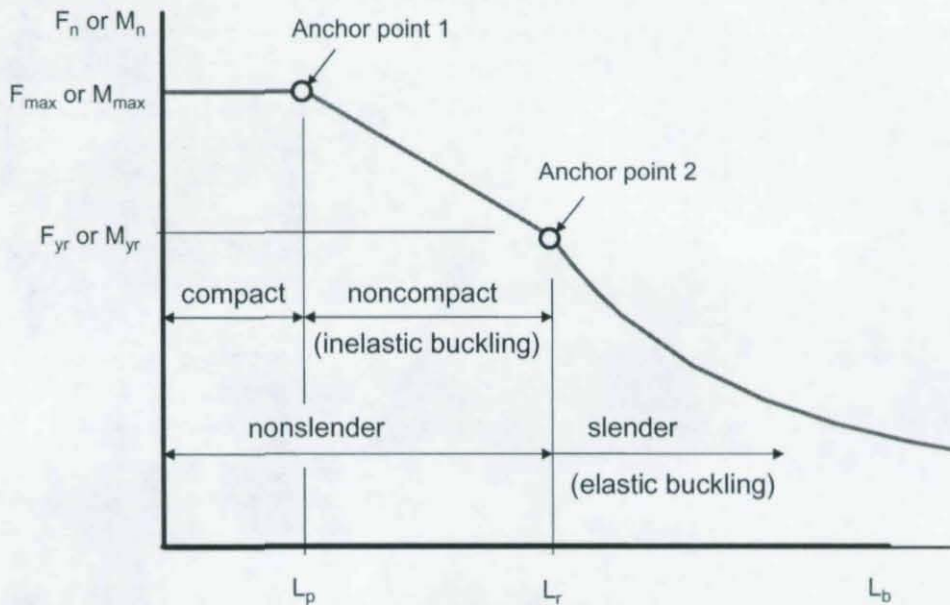
Figure 1. Basic form of the LTB provisions in AASHTO (1998 and 2004) and AISC (1999 and 2005) corresponding to uniform major-axis bending ($C_b = 1$).

ORGANIZATION

This paper first outlines the development of the recommended form of the equations for the elastic LTB resistance of I-section members and channels as well as the related equations for the unbraced length L_r. The physical significance of the parameters within these equations is

explained, and the application of the equations to channel-section members is reviewed. Comparisons are then made to the corresponding AASHTO (1998) and AISC (1999) equations, to the traditional AISC double-formula expressions, and to several other possible alternative forms of the exact beam-theory solution. The main purpose of this paper is to present the advantages of the updated equations for doubly-symmetric I-shapes and channels. The companion paper (White and Jung 2003a) addresses the application of these equations to singly-symmetric I-section members, including composite members in negative bending. Also, a simplified form of the exact beam-theory equations for singly-symmetric noncomposite I-section members is developed and evaluated in the companion paper.

DEVELOPMENT OF THE RECOMMENDED FORM OF THE ELASTIC LTB EQUATIONS

Timoshenko and Gere's (1961) fundamental equation for the elastic LTB strength of a doubly-symmetric I-beam can be expressed (for a general moment gradient case) as[1]

$$F_{cr} = \frac{C_b}{S_x} \frac{\pi}{L_b} \sqrt{\left(\frac{\pi E}{L_b}\right)^2 I_y C_w + EI_y GJ} \tag{1}$$

This equation can be written in the recommended form by first substituting

$$G = \frac{E}{2(1+v)} \tag{2}$$

factoring the term $\left(\dfrac{\pi E}{L_b}\right)^2 I_y C_w$ outside of the radical, and performing some algebraic

manipulation of the resulting second term under the radical to obtain

$$F_{cr} = C_b \frac{\pi^2 E}{L_b^2} \frac{\sqrt{I_y C_w}}{S_x} \sqrt{1 + \frac{1}{2\pi^2(1+v)} \frac{J}{\sqrt{C_w}} \frac{\sqrt{I_y}}{S_x} \frac{S_x}{\sqrt{I_y C_w}} L_b^2} \tag{3}$$

If the relationship

$$C_w = \frac{I_y h^2}{4c^2} \tag{4}$$

is substituted within the first occurrence of C_w under the radical in Eq. (3), where

---

[1] The symbols utilized in this paper are the same as those employed within AASHTO (1998 and 2004) unless noted otherwise.

$$c = \begin{cases} 1 & \text{for doubly - symmetric I - shapes} \\ \dfrac{h}{2}\sqrt{\dfrac{I_y}{C_w}} & \text{for channels} \end{cases} \tag{5}$$

is a "conversion factor" that allows the use of the same LTB equation for both I-shapes and channels, and h is the distance between the centroids of the flange elements, the elastic critical stress equation takes on the form

$$F_{cr} = C_b \frac{\pi^2 E}{L_b^2} \frac{\sqrt{I_y C_w}}{S_x} \sqrt{1 + \frac{1}{\pi^2 (1+v)} \frac{Jc}{S_x h} \frac{S_x}{\sqrt{I_y C_w}} L_b^2} \tag{6}$$

Finally, if one substitutes

$$r_t^2 = \frac{\sqrt{I_y C_w}}{S_x} \tag{7a}$$

$$X^2 = \frac{S_x h}{Jc} \tag{7b}$$

and 0.078 for the coefficient within the second term under the radical, Eq. (6) becomes

$$F_{cr} = C_b \frac{\pi^2 E}{(L_b / r_t)^2} \sqrt{1 + \frac{0.078}{X^2} (L_b / r_t)^2} \tag{8}$$

For a doubly-symmetric I-shape, the parameter r_t^2 reduces to a basic familiar form if it is recognized that

$$C_w \cong \frac{h^2 I_y}{4} \tag{9}$$

and this equation is substituted along with the definition

$$S_x = \frac{I_x}{(d/2)} \tag{10}$$

and the approximation

$$I_y \cong 2I_{yc} \tag{11}$$

into Eq. (7a). The result is

4

$$r_t^2 = \frac{I_y hd}{4I_x} \cong \frac{I_{yc} hd}{2I_x} \cong \frac{(A_{fc} b_{fc}^2 / 12) hd}{2(A_{fc} h^2 / 2 + A_w D^2 / 12 + A_{fillet} D^2)} = \frac{b_{fc}^2 / 12}{\frac{h}{d} + \frac{D^2}{hd} \frac{A_{wc}}{A_{fc}} \left(\frac{1}{3} + 2 \frac{A_{fillet}}{A_{wc}} \right)} \tag{12}$$

or

$$r_t \cong \frac{b_{fc}}{\sqrt{12 \left(\frac{h}{d} + \frac{1}{3} \frac{A_{wc}}{A_{fc}} \frac{D^2}{hd} \left(1 + 6 \frac{A_{fillet}}{A_{wc}} \right) \right)}} \tag{13}$$

where D is the depth of the web between the flange plates, d is the total section depth, $A_{fc} = b_{fc} t_{fc}$, $A_w = Dt_w$, A_{wc} is the area of the web in flexural compression, equal to $Dt_w/2$ for a doubly-symmetric I-shape, and A_{fillet} is the area of each of the four web-flange fillets. If d, h and D are assumed to be approximately equal and the influence of the web-flange fillet areas is neglected[2],

or if one considers that the product of the terms $\frac{D^2}{hd} < 1$ and $\left(1 + 6 \frac{A_{fillet}}{A_{wc}} \right) > 1$ is approximately

equal to one for all rolled I-shapes, Eq. (13) reduces to the radius of gyration of the compression flange plus one-third of the depth of the web in compression

$$r_t \cong \frac{b_{fc}}{\sqrt{12 \left(1 + \frac{1}{3} \frac{A_{wc}}{A_{fc}} \right)}} \tag{14}$$

This parameter is employed within the AASHTO (1998) and AISC (1999) provisions for design of slender-web I-girders, although Eq. (14) is not explicitly stated within these Specifications.

Equation (8), with r_t defined by Eq. (13), is for all practical purposes an exact representation of the fundamental elastic LTB strength. The only approximations invoked in writing Eq. (13) are the commonly-employed approximation associated with Eq. (9), the similar approximation of Eq. (11), and the assumption that the web-to-flange fillets are located at the bottom edge of the flange plates in the expression for I_x in Eq. (12). For the complete set of ASTM A6 W shapes, the value of r_t determined from Eq. (13) is in all cases within plus or minus one percent of the exact value given by Eq. (7a). The simpler Eq. (14) gives accurate r_t values that are less than one percent conservative relative to Eq. (7a) for beam-type W shapes with relatively narrow and relatively thin flanges (larger d/b_f and $b_f/2t_f$). However, it can be as much as 14 percent conservative relative to the exact Eq. (7a) for the heaviest column-type W shapes (small d/b_f and $b_f/2t_f$). The largest error associated with Eq. (14) is for a W14x808 section. The results are similar for welded shapes, where web-flange fillets are commonly not included in the section property calculations. For many plate girder type sections, the errors associated with the use of Eq. (14) are negligible. The authors consider the additional complexity of including the terms h/d, D^2/hd and A_{fillet}/A_{wc} in Eq. (13) to be small. Therefore, they prefer Eq. (13) relative to Eq.

---

[2] The contribution of the web-flange fillet areas is commonly neglected for welded I-sections; however, the web-flange fillet contributions are generally included in section property tables for rolled shapes, such as in AISC (2001a & b).

(14). The advantage of Eq. (14) is its familiarity and physical significance relative to the AISC (1999) and AASHTO (1998) slender-web member provisions. Equation (7a) is a fundamental and exact expression for the r_t^2 of doubly-symmetric I-shapes and channels. When Eq. (8) is employed for calculation of the elastic LTB resistance of rolled shapes, r_t can be tabulated based on Eq. (7a) to simplify the calculations.

For doubly-symmetric I-section members, Eq. (8) is a particularly useful and understandable form for the elastic LTB resistance, expressed in terms of the compression flange major-axis bending stress. All of the variables in this equation are well known in terms of their physical significance, and are readily available or easily calculated during the design process. Equation (8) shows that the fundamental elastic LTB strength is simply a function of the elastic modulus E, the slenderness $\frac{L_b}{r_t}$, the parameter $X^2 = \frac{S_x h}{Jc}$ and the moment gradient modifier C_b. As stated above, the parameter c within the term X^2 is a "conversion factor." This term captures the unique attribute of channels associated with their elastic LTB resistance, aside from their lack of symmetry, namely the difference in C_w relative to that of an I-shape. The use of Eq. (8) for both I- and channel-section members is based on the work by Hill (1954). Hill shows that the beam-theory elastic LTB equations for doubly-symmetric I-shapes are applicable for channel members, given the proper calculation of C_w for a channel. It is important however to recognize that the bracing system for such a member must be designed to resist a significant moment associated with the tendency of the channel to twist about its shear center (SSRC 1976).

The parameter X^2, equal to $\frac{S_x h}{J}$ for a doubly-symmetric I-section, has a particularly important physical significance. This term is the ratio of the bending and torsional efficiencies of the cross-section. If the approximation $d \cong h$ is used, this ratio simplifies to $\frac{2I_x}{J}$ for these shapes. A shallow I-section (small S_x and h) with wide stocky flanges (large J), will have a relatively small value for this term, whereas X^2 is typically large for a deep I-section with relatively narrow flanges. In the context of Eq. (8), the design of rolled I-section members can be facilitated by providing tabulated values of this parameter. It should be noted that this term is always greater than one.

When the second term under the radical in Eq. (8) becomes negligible relative to one, this equation reduces to the form

$$F_{cr} = C_b \frac{\pi^2 E}{(L_b / r_t)^2} \tag{15}$$

Equation (15) is utilized in AASHTO (1998) and AISC (1999) for slender-web members. The use of this form for these member types is motivated by its simplicity, the tendency of the second-term under the radical in Eq. (8) to be negligible for these types of members, and the fact that flange raking and the associated web distortion are more likely as the web slenderness becomes large (White and Jung 2003b).

If Eq. (8) is used for the elastic LTB strength, this expression can be equated to F_{yr} for the case of uniform major-axis bending ($C_b = 1$) and solved for the root of the resulting quadratic equation for L_r^2 (i.e., the equation is quartic in L_r but quadratic in L_r^2) to obtain

$$L_r = \frac{1.95 r_t}{X} \frac{E}{F_{yr}} \sqrt{1 + \sqrt{1 + 6.76 \left(\frac{F_{yr}}{E}\right)^2 X^4}} \qquad (16)$$

For slender-web I-sections, where J is taken equal to zero, the comparable result based on Eq. (15) is simply

$$L_{r(J=0)} = \pi r_t \sqrt{\frac{E}{F_{yr}}} \qquad (17)$$

The Engineer should note that although Eq. (16) is a relatively long equation involving embedded square root operations, the variables in this expression are few in number ($\frac{E}{F_{yr}}$, X and r_t) and are easily calculated or are readily available within the design process. Also, L_r is proportional to r_t. This is convenient, if the compact bracing limit L_p (the length associated with anchor point 1 in Fig. 1) is also written in terms of r_t, since in this case, all the LTB strength equations are expressed in terms of a single nondimensional parameter L_b/r_t. It is shown subsequently that r_t is a more fundamental LTB parameter than the commonly used radius of gyration of the full cross-section r_y. Furthermore, as discussed below, the consistent usage of r_t within the LTB strength expressions eliminates several significant discontinuities that occur in the AISC (1999) representations of the flexural resistance and leads to a more accurate characterization of the bending strength.

ALTERNATIVE FORM BASED ON AN EQUIVALENT RADIUS OF GYRATION r_E

There are many different ways in which Eq. (1) can be algebraically configured. Another interesting form suggested by Salmon and Johnson (1996) is obtained by rearranging Eq. (3) as

$$F_{cr} = C_b \frac{\pi^2 E}{L_b^2} \frac{\sqrt{I_y}}{S_x} \sqrt{C_w + \frac{1}{2\pi^2(1+v)} J L_b^2} \qquad (18)$$

and then equating this expression to the formula for the elastic buckling stress of an equivalent column, i.e.,

$$F_{cr} = \frac{C_b \pi^2 E}{\left(\frac{L_b}{r_E}\right)^2} \qquad (19)$$

If the resulting expression is solved for r_E^2, the result is

$$r_E^2 = \frac{\sqrt{I_y}}{S_x}\sqrt{C_w + \frac{1}{2\pi^2(1+\nu)}JL_b^2} = \frac{\sqrt{I_y}}{S_x}\sqrt{C_w + 0.039JL_b^2} \tag{20}$$

Based on this equivalent radius of gyration, the elastic LTB strength always takes the form of Eq. (19), i.e., Euler's column buckling equation modified by C_b. At first blush, this appears to be a dramatic simplification. However, this development is somewhat deceiving since the expression for r_E also contains the length L_b. The physical beam LTB behavior does not in general map all that well to the column elastic buckling equation. The authors prefer the form given by Eq. (8), where the radical containing the contribution of the St. Venant torsional stiffness is included directly within the expression for the LTB resistance.

Equations (19) and (20) are useful for gaining a better understanding of several attributes of the elastic LTB equations however. For instance, a common practice is to neglect the contribution from St. Venant torsion to the elastic LTB resistance in certain cases, or in other words, to assume $JL_b^2 = 0$ in determining the elastic LTB strength. As noted above, this assumption is invoked commonly for slender-web I-girders, partly since flange raking and the associated web distortion are more likely as the web slenderness becomes large[3]. Also, this assumption is invoked typically in the development (or motivation) of equations for the length L_p corresponding to anchor point 1 in Fig. 1, since the term $0.039\,JL_b^2$ in Eq. (20) tends to be negligible relative to C_w for the short unsupported lengths associated with $L_b = L_p$. By taking $JL_b^2 = 0$ in Eq. (20), the result is

$$r_{E(JL_b^2=0)} = r_t \tag{21}$$

COMPARISON TO THE AASHTO (1998) EQUATIONS FOR NONCOMPOSITE I-SECTIONS WITH COMPACT, NONCOMPACT AND LONGITUDINALLY-STIFFENED WEBS

The AASHTO (1998) equations corresponding to Eq. (8) also are derived directly from Eq. (1) by substituting Eqs. (2) and (9) as well as the approximation of Eq. (11). The result, after some algebraic manipulation, is

$$F_{cr} = C_b\frac{\pi E}{L_b}\frac{I_{yc}}{S_{xc}}\sqrt{\pi^2\left(\frac{h}{L_b}\right)^2 + \frac{1}{(1+\nu)}\frac{J}{I_{yc}}} = C_b\frac{3.14E}{L_b}\frac{I_{yc}}{S_{xc}}\sqrt{9.87\left(\frac{h}{L_b}\right)^2 + 0.769\frac{J}{I_{yc}}} \tag{22}$$

This expression (multiplied inappropriately by the hybrid girder factor R_h and expressed as the buckling moment $M_{cr} = R_h F_{cr} S_{xc}$) is specified in AASHTO (1998) to quantify the elastic LTB strength of noncomposite bridge I-beams and girders with compact, noncompact and longitudinally-stiffened webs.

Although Eq. (22) is strictly valid only for doubly-symmetric I-shapes, it is applied also for singly-symmetric nonslender-web I-girders in the AASHTO (1998) Specifications. The

---

[3] The influence of web distortion on the LTB strengths is considered for general doubly- and singly-symmetric I-section members in (White and Jung 2003b).

commentary of these Specifications states that Eq. (22) gives predictions within approximately 10 percent of the LTB equation for singly-symmetric I-section members provided in AISC (1999).

Equation (22) performs reasonably well for a large number of practical singly-symmetric I-shapes. However, it exhibits significant errors relative to the beam-theory based LTB strengths in certain cases (White and Jung 2003a). This is in part due to the fact that changes in the size of the tension flange and web influence the LTB strength only through the terms S_{xc}, h and J in this equation. Equation (8) also may be applied as an approximation for the elastic LTB strength of singly-symmetric I-section members. White and Jung (2003a) show that this equation, with c = 1, and r_t calculated using Eq. (13) with $A_{wc} = D_c t_w$, generally gives a more accurate approximation of the exact open-walled section beam-theory solution than Eq. (22) for singly-symmetric I-section members.

Equation (8) also has another advantage relative to Eq. (22) by virtue of the fact that as either J or L_b approaches zero, $r_{E(JL_b^2=0)} = r_t$ per Eq. (21). Therefore, Eq. (15) can be employed in the development of expressions for the length L_p shown in Fig. 1. Conversely, Eq. (22) is written most directly in terms of the compression flange radius of gyration r_{yc} as

$$F_{cr} = C_b \frac{\pi^2 E}{(L_b^2 / r_{yc}^2)} \frac{A_{fc} h}{S_{xc}} \sqrt{1 + 0.078 \frac{J}{I_{yc} h^2} L_b^2}$$ (23)

In the limit that L_b approaches zero, this equation becomes

$$F_{cr} = C_b \frac{\pi^2 E}{(L_b^2 / r_{yc}^2)} \frac{A_{fc} h}{S_{xc}}$$ (24)

Equation (8) is more fundamental in that the use of

$$r_t = r_{E(JL_b^2=0)} = r_{yc} \sqrt{\frac{S_{xc}}{A_{fc} h}}$$ (25)

gives the fundamental LTB form of Eqs. (15) and (19) for a doubly-symmetric I-shape in the limit that $0.078 J \left(\frac{L_b}{r_t} \right)^2$ becomes small relative to $S_x h \cong 2I_x$ (see the last term under the radical in Eq. (8)). The reader should note that r_{yc} is the radius of gyration of the compression flange alone, equal to $b_{fc}/\sqrt{12}$ for a rectangular flange plate. This should be contrasted with the definition of r_t given by Eq. (14).

AASHTO (1998) does not specify an equation for the term L_r in the context of its use of Eq. (22). Rather the AASHTO (1998) Specifications use the elastic LTB strength for all moment levels less than the yield moment M_y multiplied by the hybrid girder factor R_h. The AASHTO (2004) provisions provide a more accurate representation of the LTB resistance by adopting the form shown in Fig. 1.

9

COMPARISON TO THE AISC (1999) EQUATIONS FOR DOUBLY-SYMMETRIC I- AND CHANNEL-SECTION MEMBERS

Two forms of the exact beam-theory equations for elastic LTB of doubly-symmetric open-walled sections are specified in AISC (1999), Eq. (1) multiplied by S_x, and

$$M_{cr} = \frac{C_b S_x X_1 \sqrt{2}}{L_b / r_y} \sqrt{1 + \frac{X_1^2 X_2}{2(L_b / r_y)^2}} \tag{26}$$

where

$$X_1 = \frac{\pi}{S_x} \sqrt{\frac{EGJA}{2}} \tag{27}$$

and

$$X_2 = 4 \frac{C_w}{I_y} \left(\frac{S_x}{GJ}\right)^2 \tag{28}$$

The primary reason for Eq. (26) is the use of L_b/r_y as a nondimensional slenderness parameter in writing the elastic LTB strength. The original form given by Eq. (1) is simpler. The authors recommend Eq. (8) as a simple LTB strength expression based on the slenderness L_b/r_t.

AISC (1999) gives a single expression for L_r, which is derived from Eq. (26) in a fashion similar to the development of Eq. (16) from Eq. (8):

$$L_r = \frac{r_y X_1}{F_{yr}} \sqrt{1 + \sqrt{1 + X_2 F_{yr}^2}} \tag{29}$$

As noted in the Introduction, the physical significance of the parameters X_1 and X_2 is difficult to understand. The recommended alternative to this equation, Eq. (16), involves the three parameters $\frac{E}{F_{yr}}$, X and r_t. As discussed previously, the physical significance of each of these parameters is easy to understand. Furthermore, the values for X^2 and r_t can be tabulated for standard I-shapes, similar to the tabulation of X_1 and X_2 in AISC (2001a and b).

In the limit that J or L_b approaches zero, Eq. (1) can be expressed directly as

$$F_{cr} = C_b \frac{\pi^2 E}{L_b^2} \frac{\sqrt{I_y C_w}}{S_x} \tag{30}$$

By substituting Eq. (9), this equation may be written as

$$M_{cr} = C_b \frac{\pi^2 E \frac{I_y}{2}}{L_b^2} \frac{h}{S_x} = C_b \frac{\pi^2 E}{(L_b / r_y)^2} \frac{Ah}{2S_x} \tag{31}$$

Similar to the development in the previous section, Eq. (8) is more fundamental in that the use of

$$r_t = r_{E(JL_b^2 = 0)} = r_y \sqrt{\frac{2S_x}{Ah}} \tag{32}$$

gives the basic LTB form of Eqs. (15) and (19) for a doubly-symmetric I-shape in the limit that $0.078J \left(\frac{L_b}{r_t} \right)^2$ becomes small relative to $S_x h \cong 2I_x$ in Eq. (8). The reader should note that r_y is the radius of gyration of the full doubly-symmetric cross-section. This term may be expressed as $\dfrac{b_{fc}}{\sqrt{12 \left(1 + \dfrac{A_{wc}}{A_{fc}} \right)}}$ for a rectangular flange plate. It is interesting to compare this expression to the form given by Eq. (14) for r_t.

One way in which the equations for L_p (the length corresponding to anchor point 1 in Fig. 1) are often motivated is to replace the elastic modulus by the strain-hardening modulus E_s within Eq. (31) (Galambos 1968; McGuire 1968; Salmon and Johnson 1996). This is based on the assumption that substantial plastic bending deformations are developed throughout the cross-section prior to LTB. If Eqs. (24) or (31) are utilized within this context, an assumed value must be introduced for the extraneous parameters $\frac{A_{fc} h}{S_{xc}}$ or $\frac{Ah}{2S_x}$. Conversely, if Eq. (15) is employed as the base equation, L_p can be expressed directly as (using $C_b = 1$)

$$L_p = r_t \sqrt{\frac{\pi^2 E_s}{mF_y}} \tag{33}$$

where m is a multiple of the yield strength corresponding to the compression flange state within the heavily plastified cross-section. If the approximations $E_s = 0.03E$ and $m = 1.12$ are introduced, this expression becomes

$$L_p = 0.51 r_t \sqrt{\frac{E}{F_y}} \tag{34}$$

As discussed with the developments in (Galambos 1968) and (McGuire 1968), the unbraced length does not need to be restricted this severely for members to be able to develop substantial plasticity prior to the nominal strength being influenced by LTB. Futhermore, it should be emphasized that the above derivations are primarily for motivational purposes. The true physical aspects of the LTB response of heavily plastified members are significantly more complex than implied by the above idealizations. White and Jung (2004) show that the equation

11

$$L_p = 1.1 r_t \sqrt{\frac{E}{F_y}}$$
(35)

gives the best fit to the data for anchor point 1 from 277 experimental LTB tests of rolled and welded I-section members in uniform bending.

An important advantage of the use of r_t in the L_p equation is that it eliminates several discontinuities that occur within the AISC (1999) provisions. AISC (1999) Appendix F uses the radius of gyration of the compression flange alone, r_{yc}, in writing the L_p limit for singly-symmetric I-section members. This results in an abrupt increase in L_p if a doubly-symmetric section is made slightly singly-symmetric. Appendix F of AISC (1999) uses r_y within its L_p equation for doubly-symmetric I-shapes. Furthermore, Appendix G specifies r_t for all types of slender-web I-sections. This results in a discontinuity in L_p as the web transitions from a noncompact to a slender element. If r_t is employed for singly-symmetric I-section members that have the same web and compression flange, but have larger tension flanges of various sizes, the L_p limit tends to decrease with increasing monosymmetry. This characteristic follows experimentally observed trends (White and Jung 2004; White and Kim 2004), which indicate that more restrictive limits are needed on the length L_p corresponding to Anchor Point 1 (Fig. 1), for these types of members to have a similar level of reliability compared to other types of I-section members. In addition, the fact that r_t is associated solely with the compression portion of the I-section allows composite I-section members in negative bending to be handled in a simplified fashion using the same equations as for singly-symmetric I-section members. White and Jung (2003a) address this issue in more detail. Lastly, the use of r_t in Eq. (35) is consistent with the use of the ratio M_{max}/M_{cr} in the definition of unbraced length limits comparable to L_p in the Canadian (CSA 2001), Australian (SAA 1998), Eurocode (CEN 1993) and British (BSI 1990) Standards.

COMPARISON TO THE TRADITIONAL DOUBLE-FORMULA APPROACH FOR DOUBLY-SYMMETRIC I-SECTION MEMBERS

As discussed in (SSRC 1976), Eq. (1) also may be written in the forms

$$F_{cr} = \frac{C_b}{S_{xc}} \frac{\pi \sqrt{EI_y GJ}}{L_b} \sqrt{1 + \frac{EC_w}{GJ}\left(\frac{\pi}{L_b}\right)^2}$$
(36)

and

$$F_{cr} = \frac{C_b h}{S_{xc}} \frac{\pi^2 E\left(\frac{I_y}{2}\right)}{L_b^2} \sqrt{1 + \frac{GJ}{EC_w}\left(\frac{L_b}{\pi}\right)^2}$$
(37)

For shallow (small d/b_f) and/or stocky cross-section members, the elastic LTB resistance is dominated by the St. Venant torsional stiffness and the value of the radical in Eq. (36) approaches unity. In this case, this equation, written in terms of moment, can be simplified to

12

$$M_{cr} \cong \frac{1.95 C_b E \sqrt{I_y J}}{L_b} \tag{38}$$

Similarly, for deep (large d/b_f) thin-walled I-girders, the elastic LTB resistance is dominated by the stiffness associated with the nonuniform or warping torsion, and the radical in Eq. (37) approaches unity. In this case, Eq. (37), written in terms of moment, can be simplified to

$$M_{cr} = C_b h \frac{\pi^2 E I_{yc}}{L_b^2} \tag{39}$$

The traditional AISC ASD double-formula equations for the elastic LTB resistance of doubly-symmetric I-section members are obtained by substituting the basic expressions for I_y, J and I_{yc} and introducing the additional approximations of: (1) $d \cong 2b_f$ and (2) $t_w \cong 2t_f/3$. Equations (38) and (39) are retained here since they allow evaluation of the fundamental approximations of $C_w/L_b^2 = 0$ and $JL_b^2 = 0$ in writing these equations. In the traditional ASD double-formula method, the elastic LTB resistance is taken as the larger of the values from these two approximations.

Figure 2 shows the nature of the above approximation in terms of the resulting predicted M_{cr}/M_y at $L_b = L_{r(exact)}$, where M_y is the yield moment $F_y S_{xc}$, and $L_{r(exact)}$ is based on Eq. (16) using $F_y = 50$ ksi (345 MPa) and $F_{yr} = 0.7F_y$, as specified for doubly-symmetric nonhybrid shapes in AASHTO (2004) and AISC (2005). The exact value of M_{cr}/M_y is 0.7 for all the members considered in this plot. The data points within Fig. 2 correspond to the complete set of ASTM A6 rolled wide-flange shapes listed in the AISC (2001b) Shapes Database. Figure 3 shows the related approximations for the ratio of the approximate to the exact values of L_r, $L_{r(approx)}/L_{r(exact)}$, obtained using Eqs. (38) and (39) (by setting F_{cr} to $0.7F_y$ and solving for the corresponding length). The following observations can be made from these plots:

- The fundamental errors in the double-formula based strengths are highly correlated with the parameter X^2 of the recommended elastic LTB equations (8) and (16).

- The conservative approximation of L_r associated with Eq. (38) is generally less than 10 percent for $X^2 \leq 350$

- The conservative approximation of L_r associated with Eq. (39) is generally less than 10 percent for $X^2 \geq 1500$

- For values of X^2 between 350 and 1500, the conservative errors in L_r associated with the double-formula approach are in general larger than 10 percent. The largest error is 21 percent (i.e., $L_{r(approx)} = 0.79 L_{r(exact)}$ at $X^2 = 640$, which is the value of this term where the L_r values predicted based on Eqs. (38) and (39) are the same.

- Although the approximation of Eq. (38) is quite good for column-type wide-flange sections (i.e., $d/b_f \cong 1$) with the stockiest plate components, in general the use of this equation results in a significant but needless conservative approximation of the true M_{cr} or L_r values.

13
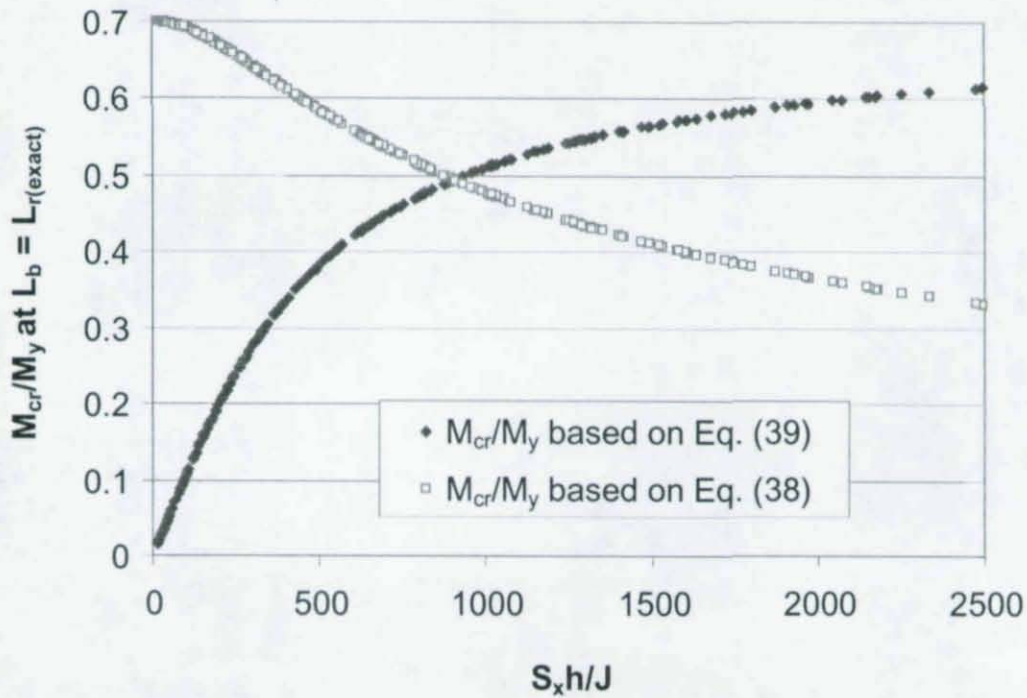
Figure 2. Ratio of the critical moment obtained from Eqs. (38) and (39) to the yield moment M_y at L_b equal to the exact value of L_r from Eq. (16) for $F_{yr} = 0.7F_y$ and $F_y = 50$ ksi (345 MPa) for the complete set of ASTM A6 W shapes. The exact M_{cr}/M_y is equal to 0.7 for all the points in this plot.
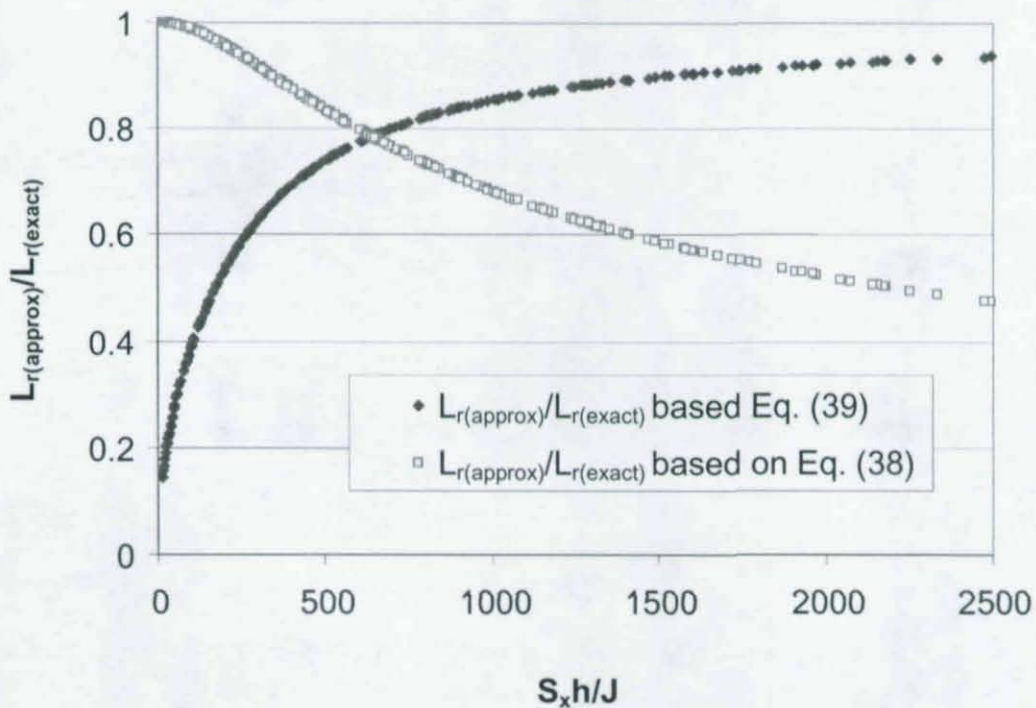
Figure 3. Ratio of the values of L_r based on Eqs. (38) and (39) to the exact value from Eq. (16) for $F_{yr} = 0.7F_y$ and $F_y = 50$ ksi (345 MPa) for the complete set of ASTM A6 W shapes.

14

- Although the approximation by the use of Eq. (39) in the calculation of L_r is less than 10 percent conservative for $X^2 \geq 1500$, the conservative error is still six percent at $X^2 = 2500$. Therefore, assuming that the reduction in the LTB resistance due to potential web distortion is not an issue, it can be concluded that Eq. (39) results in a significant and needless conservative error in the elastic LTB resistances. Also, the Engineer should note that for unbraced lengths larger than $L_b = L_r$, the conservative error associated with the use of Eq. (39) is larger.

Figures 4 and 5 show the variation in M_{cr}/M_y from Eqs. (38) and (39) at $L_b = L_{r(exact)}$ versus the cross-section aspect ratio d/b_f for the complete set of all ASTM A6 W shapes. The significance of the parameter d/b_f is that cross-sections that have a larger d/b_f tend to work more efficiently for problems involving flexure only, while cross-sections with d/b_r close to 1.0 tend to work better as columns. Figure 4 shows that even for column-type W sections (i.e., $d/b_f \cong 1$), where Eq. (38) would tend to govern in the double-formula approach, the conservative error in using Eq. (38) can be greater than 10 percent. The more conservative predictions for a given d/b_f in Fig. 4 tend to occur for sections that have thinner flange and web plates. Furthermore, Fig. 5 shows that even for beam-type W sections with $d/b_f > 3$, the use of Eq. (39) alone can result in conservative errors that are larger than 50 percent. The more conservative predictions in this case tend to occur for sections that have highly stocky flanges. Also, it should be noted that the conservative error associated with the application of Eq. (15) to these types of rolled wide-flange sections is similar to that shown in Fig. 5.

The use of the single elastic LTB expression given by Eq. (8) is in general significantly more accurate, and in addition the use of this equation is more straightforward compared to calculating the resistances from the two separate double-formula equations and then taking the larger of the two values. Also, it is relatively easy to understand the physical significance of the terms in Eqs. (8) and (16). Furthermore, these equations reduce naturally to the forms generally employed for slender-web members, i.e., Eqs. (15) and (17), simply by taking $J = 0$. Equations (15) and (17) should be used for slender-web members, where the influence of the St. Venant torsional stiffness is typically small and web distortion effects are of a potential concern. Lastly, Eqs. (8) and (16) can be applied for all types of I-sections and channels, including composite I-section members in negative bending. This is not the case for the AASHTO (1998) I_{yc}-based equation or the AISC (1989) double-formula equations.

Appendix A evaluates when the simple Eq. (17) can be employed for L_r with small (less than 10 percent) conservative error in terms of the cross-section dimensional parameters. As noted above, the conservative error associated with the use of $J = 0$ is generally larger for $L_b > L_r$. Therefore, Eq. (8) should be used in general for calculating the elastic LTB strength of members with compact or noncompact webs.

SUMMARY

The elastic LTB strength of doubly-symmetric I-section members and channels can be expressed in the exact but simple and easily understood form given by Eq. (8):

$$F_{cr} = C_b \frac{\pi^2 E}{(L_b / r_t)^2} \sqrt{1 + \frac{0.078}{X^2} (L_b / r_t)^2} \tag{8}$$
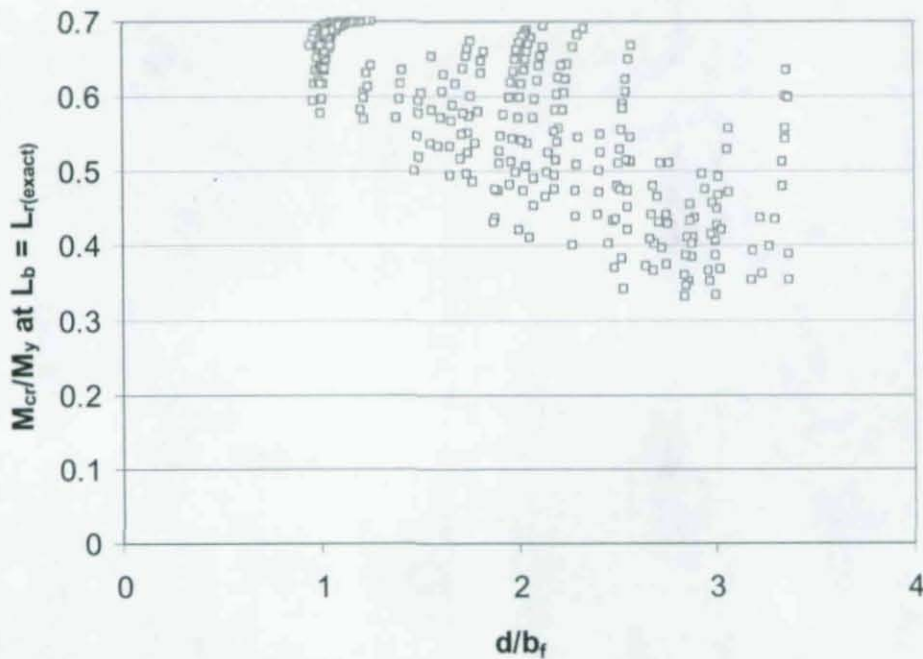
Figure 4. Ratio of the critical moment obtained from Eq. (38) (based on neglecting the warping rigidity EC_w) to the yield moment M_y, at L_b equal to the exact value of L_r from Eq. (16) for $F_{yr} = 0.7F_y$ and $F_y = 50$ ksi (345 MPa) for the complete set of ASTM A6 W shapes. The exact M_{cr}/M_y is equal to 0.7 for all the points in this plot.
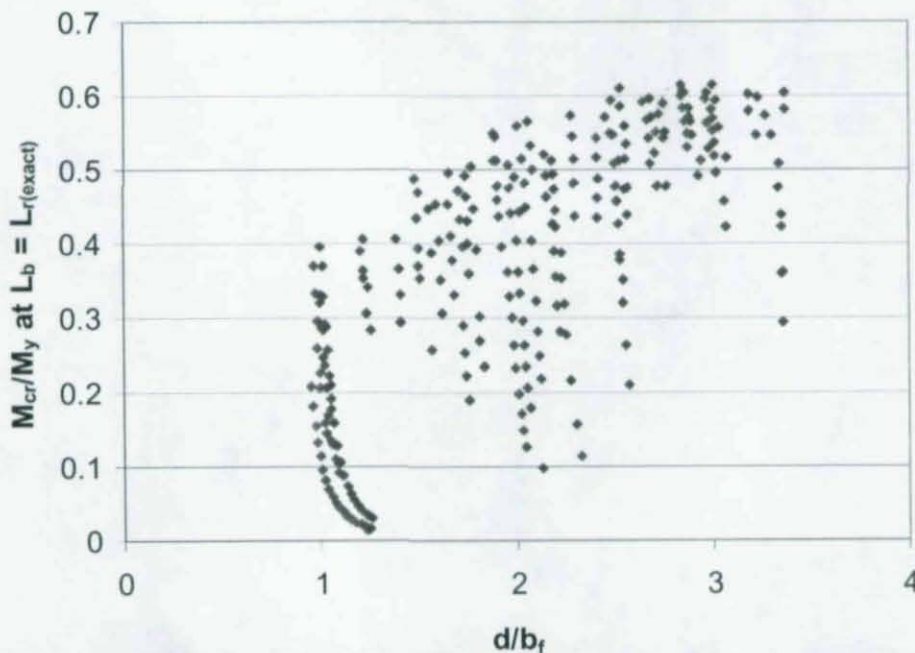
Figure 5. Ratio of the critical moment obtained from Eq. (39) (based on neglecting the St. Venant torsional rigidity GJ) to the yield moment M_y, at L_b equal to the exact value of L_r from Eq. (16) for $F_{yr} = 0.7F_y$ and $F_y = 50$ ksi (345 MPa) for the complete set of ASTM A6 W shapes. The exact M_{cr}/M_y is equal to 0.7 for all the points in this plot.

This equation shows that the elastic LTB resistance of these types of members depends on the moment gradient factor C_b, the elastic modulus E, the slenderness parameter L_b/r_t, and the ratio of the torsional and bending efficiencies of the cross-section $X^2 = \dfrac{S_x h}{Jc}$. This last term reduces approximately to $\dfrac{2I_x}{J}$ for a doubly-symmetric I-shape. All of these variables are well known in terms of their physical significance, and are readily available or are easily calculated during the design process. The use of Eq. (8) in the design of rolled I-shapes and channels can be facilitated by tabulating the values of r_t and X^2, where r_t may be calculated exactly for doubly-symmetric I-shapes and channels from Eq. (7a) and c is a conversion factor for channels given by Eq. (5). As discussed by White and Jung (2003a), Eq. (8) can also be used as an accurate approximation for the elastic LTB strength of a wide range of singly-symmetric I-section members, including composite members in negative bending, but with r_t given by Eq. (13). Equation (8) also has the advantage that it reduces to the elastic LTB equation for slender-web I-section members in AISC (1999) and AASHTO (1998) simply by substituting J = 0, i.e.,

$$F_{cr} = C_b \frac{\pi^2 E}{(L_b / r_t)^2} \tag{15}$$

The unbraced length corresponding to the transition from inelastic to elastic LTB corresponding to Eq. (8), L_r, is given by Eq. (16):

$$L_r = \frac{1.95 r_t}{X} \frac{E}{F_{yr}} \sqrt{1 + \sqrt{1 + 6.76 \left(\frac{F_{yr}}{E}\right)^2 X^4}} \tag{16}$$

This equation is similar in form to the corresponding exact equation in AISC (1999) (Eq. (29)), but is based on the more fundamental parameters discussed above. The comparable equation for slender-web members reduces to the particularly simple form given by Eq. (17):

$$L_{r(J=0)} = \pi r_t \sqrt{\frac{E}{F_{yr}}} \tag{17}$$

The above recommended equations are compared to various other exact and approximate forms for the elastic LTB strength of doubly-symmetric I-section members and channels. The paper shows that the radius of gyration r_t, given exactly by Eq. (7a) for doubly-symmetric I-shapes and channels and closely approximated by Eq. (13) for I-section members, is more fundamental to the LTB problem than r_y or r_{yc}. In the limit that $0.078J \left(\dfrac{L_b}{r_t}\right)^2$ becomes negligible relative to $S_x h \cong 2I_x$ in the last term of Eq. (8), the elastic LTB strength reduces to the form of Euler's column buckling equation, but with the radius of gyration taken as r_t. Conversely, additional terms remain within the elastic LTB strength formulas at this limit when r_y or r_{yc} are used.

The paper also shows that, although the traditional double-formula approach gives reasonable results at the extreme limits of shallow stocky column-type I-sections and deep narrow-flange beam-type I-sections, the two separate equations used in this approach give quite conservative answers for a large percentage of rolled I-shapes. The errors associated with the double-formula approach are strongly correlated with the bending to torsional efficiency ratio X^2.

Detailed assessment of the cross-section dimensional parameters for which the simplest approximate equation for L_r (Eq. (17)) is less than 10 percent conservative are evaluated in Appendix A. In general, the St. Venant torsional stiffness J should be included for accurate calculation of the elastic LTB resistance in compact- and noncompact-web members for lengths larger than L_r. This is because the conservative errors associated with the use of J = 0 are larger for increasing values of the unbraced length L_b.

The companion paper (White and Jung 2003a) considers an ad hoc extension of the recommended elastic LTB equations, similar in concept to the development and use of comparable elastic LTB equations for singly-symmetric I-shapes in AASHTO (1998). This ad hoc extension is useful since only one set of equations is then needed to handle all types of I-section members and channels, including lateral buckling of the bottom flange of composite I-section members in negative bending. The recommended equations give improved accuracy relative to the AASHTO (1998) equations for general I-shapes. The companion paper also develops and evaluates a simplified form of the exact beam-theory equations for singly-symmetric I-section members. Considerations pertaining to the calculation of the St. Venant torsional stiffness J for general I-shapes as well as reductions in the elastic LTB resistance due to web distortion are addressed by White and Jung (2003b).

ACKNOWLEDGEMENTS

REFERENCES

AASHTO (1998). *AASHTO LRFD Bridge Design Specifications 2nd Edition with 1999, 2000 and 2001 Interims*, American Association of State and Highway Transportation Officials, Washington D.C.

AASHTO (2004). *AASHTO LRFD Bridge Design Specifciations, 3rd Edition*, American Association of State and Highway Transportation Officials, Washington, D.C.

AISC (2005). *Specification for Structural Steel Buildings*, American Institute of Steel Construction, Chicago, IL (to appear).

AISC (2001a). Manual of Steel Construction, Load and Resistance Factor Design, 3rd Ed., American Institute of Steel Construction, Inc., Chicago, IL.

AISC (2001b). Shapes Database, Version 3.01, American Institute of Steel Construction, Chicago, IL.

AISC (1999). *Load and Resistance Factor Design Specification for Structural Steel Buildings*, American Institute of Steel Construction, Chicago, IL, 292 pp.

AISC (1989). *Specification for Structural Steel Buildings: Allowable Stress Design and Plastic Design*, 9th Ed., American Institute of Steel Construction, Chicago, IL.

Clark, J.W. and Hill, H.N. (1960). "Lateral Buckling of Beams," *Journal of the Structural Division*, ASCE, 86(ST7), 175-196.

CEN (1993). *Eurocode 3: Design of Steel Structures, Part1.1 – General Rules and Rules for Buildings*, ENV 1992-1-1, European Committee for Standardization, Brussels, Belgium.

CSA (2001). *Limit States Design of Steel Structures*, CAN/CSA-S16-01, Canadian Standards Association, Toronto, Ontario, Canada.

de Vries, K. (1947). "Strength of Beams as Determined by Lateral Buckling," *Transactions*, ASCE, 112, 1245-1271.

Galambos, T.V. (1968). *Structural Members and Frames*. Prentice Hall, Englewood Cliffs, NJ, 373 pp.

Hill, H.N. (1954). "Lateral Buckling of Channels and Z-Beams," *Transactions*, ASCE, 119, p. 829.

Hoadley, P.W. (1991). "Practical Significance of LRFD Beam Buckling Factors," *Journal of Structural Engineering*, 117(3), 988-996.

McGuire, W. (1968). *Steel Structures*. Prentice Hall, N.J., 1112 pp.

SAA (1998). *Steel Structures*, AS4100-1998, Standards Association of Australia, Australian Institute of Steel Construction, Sydney, Australia.

Salmon, C.G. and Johnson, J.E. (1996). *Steel Structures, Design and Behavior*, 4th Ed., Prentice Hall, NJ, 1024 pp.

SSRC (1998). *Guide to Stability Design Criteria for Metal Structures*, T.V. Galambos (ed.), Structural Stability Research Council, Wiley Interscience, New York, NY, 911 pp.

SSRC (1976). *Guide to Stability Design Criteria for Metal Structures*, B.G. Johnston (ed.), Structural Stability Research Council, Wiley Interscience, New York, NY, 616 pp.

Timoshenko, S.P. and Gere, J.M. (1961). *Theory of Elastic Stability*, McGraw-Hill, New York, NY, 541 pp.

White, D.W. and Jung, S.-K. (2003a). "Simplified Lateral-Torsional Buckling Equations for Singly-Symmetric I-Section Members," Report 24b, School of Civil and Environmental Engineering, Georgia Insitutute of Technology, Atlanta, GA.

White, D.W. and Jung, S.-K. (2003b). "Effect of Web Distortion on the Buckling Strength of Noncomposite Discretely-Braced I-Beams," Structural Engineering, Mechanics and Materials Report No. 24c, School of Civil and Environmental Engineering, Georgia Insitutute of Technology, Atlanta, GA.

White, D.W. and Jung, S.-K. (2004). "Unified Flexural Resistance Equations for Stability Design of Steel I-Section Members – Uniform Bending Tests," Structural Engineering, Mechanics and Materials Report No. 28, School of Civil and Environmental Engineering, Georgia Institute of Technology, Atlanta, GA.

White, D.W. and Kim, Y.D. (2004). "Unified Flexural Resistance Equations for Stability Design of Steel I-Section Members – Moment Gradient Tests," Structural Engineering, Mechanics and Materials Report No. 29, School of Civil and Environmental Engineering, Georgia Institute of Technology, Atlanta, GA.

APPENDIX A – CONSERVATIVE ERROR ASSOCIATED WITH THE USE OF J = 0 IN CALCULATING L_r FOR COMPACT- AND NONCOMPACT-WEB I-SECTIONS

The parameter L_r is the unsupported length at the transition between the elastic and inelastic LTB strength curves in AASHTO (1998) and AISC (1999). As noted in the paper, the equations for L_r are derived in general by equating the base elastic LTB strength F_{cr} to the compression flange stress corresponding to the onset of significant cross-section inelasticity, F_{yr}. Equation (16) is derived in this fashion based on the recommended general form for the elastic LTB resistance (Eq. (8)), and Eq. (17) is obtained in this fashion from Eq. (15) for slender-web members, where J is taken equal to zero. Since Eq. (16) involves embedded square root operations, yet Eq. (17) is extraordinarily simple, it is interesting to investigate to what extent the inclusion of a finite J in Eq. (16) increases the value of L_r relative to that computed from Eq. (17). In this appendix, the percent difference between the L_r value determined by Eq. (16) compared to that determined by Eq. (17) is derived analytically.

One can observe that the ratio of the strengths predicted by Eqs. (8) and (15) depends solely on the term $\dfrac{0.078}{X^2}(L_b / r_t)^2$ inside the radical of Eq. (8). With some algebraic manipulation, the ratio X^2 can be expressed in terms of the nondimensional parameters D/b_{fc}, b_{fc}/t_{fc}, D/t_w, and t_{ft}/t_{fc} for a general I-shape as

$$X^2 = \frac{S_{xc}h}{J} = \frac{(h/d)[(d^3 - D^3)b_{fc} + D^3 t_w]}{2(b_{fc}t_{fc}^3 + b_{ft}t_{ft}^3 + Dt_w^3)} = \frac{(h/d)[\{(d/D)^3 - 1\} + t_w/b_{fc}]}{2[(t_{fc}/D)^3 + (b_{ft}/b_{fc})(t_{ft}/D)^3 + (D/b_{fc})(t_w/D)^3]}$$

$$= \frac{(h/d)\left[\left\{\left(1 + \dfrac{1}{(D/b_{fc})(b_{fc}/t_{fc})} + \dfrac{(t_{ft}/t_{fc})}{(D/b_{fc})(b_{fc}/t_{fc})}\right)^3 - 1\right\} + \dfrac{(D/b_{fc})}{(D/t_w)}\right]}{2\left[\dfrac{1}{(b_{fc}/t_{fc})^3(D/b_{fc})^3} + \dfrac{(b_{ft}/b_{fc})(t_{ft}/t_{fc})^3}{(b_{fc}/t_{fc})^3(D/b_{fc})^3} + \dfrac{(D/b_{fc})}{(D/t_w)^3}\right]}$$

$$\cong \frac{\left[\left\{\left(1 + \dfrac{1 + (t_{ft}/t_{fc})}{(D/b_{fc})(b_{fc}/t_{fc})}\right)^3 - 1\right\} + \dfrac{(D/b_{fc})}{(D/t_w)}\right]}{\left[2 + \dfrac{1 + (t_{ft}/t_{fc})}{(D/b_{fc})(b_{fc}/t_{fc})}\right]\left[\dfrac{1 + (b_{ft}/b_{fc})(t_{ft}/t_{fc})^3}{(b_{fc}/t_{fc})^3(D/b_{fc})^3} + \dfrac{(D/b_{fc})}{(D/t_w)^3}\right]} \tag{40}$$

It should be noted that the final approximation in this equation is obtained by assuming

$$d/h \cong h/D = \left[1 + \frac{t_{fc}/2}{D} + \frac{t_{ft}/2}{D}\right] \tag{41}$$

If Eq. (40) is substituted into Eq. (16) for X^2, and then Eq. (16) is divided by Eq. (17), the result is a basic equation for the ratio of the L_r values computed with and without the inclusion of J. Figure 6 shows a plot of the 10 percent conservative "error" curves in L_r associated with the use of Eq. (17) instead of Eq. (16). That is, each of the curves in Fig. 6 gives the values of b_f/t_f and D/t_w associated with 10 percent conservative error in L_r for a given value of D/b_f. For each of the values of D/b_f, any points (D/t_w, b_f/t_f) that fall above and to the right of the corresponding curve have conservative errors smaller than 10 percent. This figure is based on $F_y = 50$ ksi (345 MPa) and $F_{yr} = 0.7F_y$, which is the specified value of F_{yr} for doubly-symmetric nonhybrid shapes in AASHTO (2004) and AISC (2005).
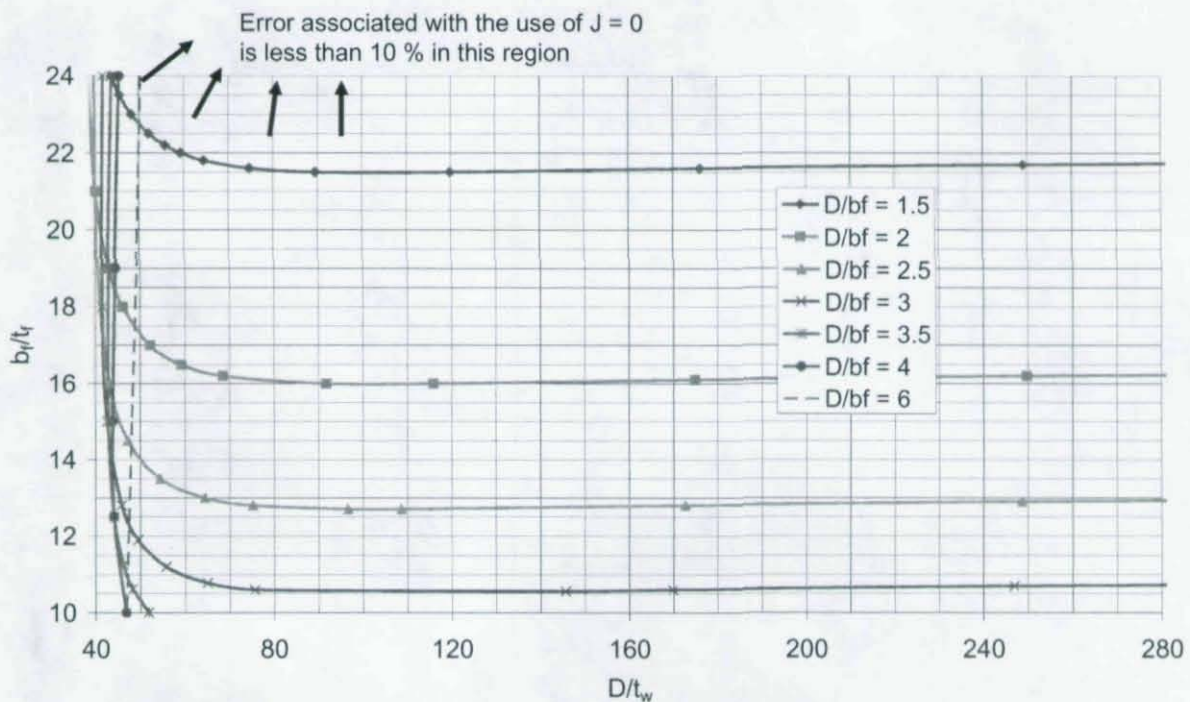
Figure 6. Curves for 10 percent conservative error in L_r associated with the use of $J = 0$, plotted as a function of D/b_f, b_f/t_f and D/t_w based on Eqs. (16) and (17), $F_{yr} = 0.7F_y$, $F_y = 50$ ksi (345 MPa).

One can observe from Fig. 6 that for $D/b_f \geq 3$, $D/t_w \geq 50$ and $b_f/t_f \geq 11$ ($b_f/2t_f = 5.5$), the influence of J on the value of L_r is essentially always less than 10 percent. This is significant since many welded beam and girder type cross-sections will satisfy these limits. Even when $D/b_f = 2.5$, which is likely to be smaller than the value of D/b_f for many welded I-girders, the error in L_r associated with neglecting J is less than 10 percent essentially if $b_f/t_f \geq 13$ and $D/t_w \geq 50$. For $D/b_f \geq 3.5$, the error in L_r associated with the assumption of $J = 0$ is less than 10 percent if $b_f/t_f \geq 10$ (or $b_f/2t_f \geq 5$) and $D/t_w \geq 50$. Therefore, practically speaking, the error in L_r associated with the use of $J = 0$ is less than 10 percent for most bridge-girder type proportions. For larger F_y (and F_{yr}) values than those on which Fig. 6 is based, the horizontal portion of the 10

21

percent error curves tends to shift downward, and the vertical portion of the curves for large D/b_f (e.g., $D/b_f = 6$) tends to shift slightly to the right.

For rolled beam type wide-flange sections, it can be stated that the conservative error in L_r caused by using $J = 0$ will typically be greater than 10 percent, although not much greater for many light beam-type wide-flange sections. This can be inferred from Fig. 6, although it is not illustrated directly by the plot. Figure 5 shows however that for some beam-type wide-flange sections (e.g., sections with heavy flanges), the conservative error associated with the use of Eqs. (15) and (17) is substantial. Furthermore, Fig. 6 shows that for typical column type rolled or welded I-shapes, which tend to have D/b_f close to one and D/t_w less than 50, the conservative error in L_r associated with the use of $J = 0$ is always larger than 10 percent. For many column-type cross-sections, this error is in fact significantly larger than 10 percent. This attribute is illustrated by the conservative nature of the curve for $L_{r(approx)}/L_{r(exact)}$ based on Eq. (39) for small values of $X^2 = \dfrac{S_x h}{J}$ in Fig. 3. It is also illustrated by the small values for M_{cr}/M_y at $L_b = L_{r(exact)}$ and $d/b_f \cong 1$ in Fig. 5. Figure 6 shows that for doubly-symmetric I sections with D/t_w less than about 40, the increase in L_r due to the St. Venant torsional rigidity is always greater than 10 percent.

Based on Fig. 6, it can be argued that it is often reasonable to neglect J in calculating L_r for welded I-girders. However, the error associated with the assumption of $J = 0$ becomes much larger for unsupported lengths larger than L_r. That is, for long unsupported lengths typical of conditions which may exist during construction, the additional strength gained by the inclusion of J in Eq. (8) compared to that predicted by Eq. (15) based on $J = 0$ can be substantial. Therefore, it is recommended that in general Eqs. (8) and (16) should be utilized in calculating the strength of compact- and noncompact-web I-section members. Use of Eq. (8) for F_{cr} and Eq. (17) for L_r would lead to a discontinuity in the elastic and inelastic LTB strength curves at the transition point, i.e., anchor point 2 in Fig. 1.

APPENDIX B – NOTATION

A	Total cross-sectional area, in^2 (mm^2)
A_{fc}	Area of compression flange, in^2 (mm^2)
A_{fillet}	Area of each of the two web-to-compression flange fillets, generally taken equal to zero for welded I-shapes, in^2 (mm^2)
A_w	Area of web, Dt_w, in^2 (mm^2)
A_{wc}	Area of web in flexural compression, $D_c t_w$, in^2 (mm^2)
C_b	Moment-gradient factor for lateral-torsional buckling
C_w	Warping constant, in^6 (mm^6)
D	Depth of the web; clear distance between the flange plates, in (mm)
D_c	Depth of the web in compression; distance from the cross-section centroid to the inside face of the compression flange, in (mm)
E	Modulus of elasticity of steel, 29 000 ksi (200 000 MPa)
E_s	Strain-hardening modulus of steel, ksi (MPa)
F_{cr}	Elastic critical stress, ksi (MPa)
F_{max}	Maximum potential flexural resistance in terms of the compression flange stress, ksi (MPa)
F_n	Nominal flexural resistance in terms of the compression flange stress, ksi (MPa)
F_y	Specified minimum yield stress, ksi (MPa)
F_{yr}	Compression flange flexural stress corresponding to the nominal onset of yielding at the extreme fibers in compression or tension, including compression flange residual stress effects

G	Shear modulus of elasticity of steel, 11 200 ksi (77 220MPa)
I_x	Moment of inertia about the major axis of bending, in^4 (mm^4)
I_y	Moment of inertia about the minor-axis of bending, in^4 (mm^4)
I_{yc}	Moment of inertia of the compression flange about the plane of the web, in^4 (mm^4)
J	St. Venant torsional constant, in^4 (mm^4)
L_b	Laterally unbraced length; length between points braced against lateral displacement of the compression flange, or between points braced to prevent twist of the cross-section, in (mm)
L_p	Limiting laterally unbraced length to achieve the maximum potential flexural resistance of the section, uniform moment case ($C_b = 1.0$), in (mm)
L_r	Limiting laterally unbraced length to achieve the onset of yielding in uniform bending ($C_b = 1.0$) at the extreme fibers in compression or tension, with consideration of compression flange residual stress effects, in (mm)
M_{cr}	Elastic buckling moment, kip-in (N-mm)
M_n	Nominal flexural resistance, kip-in (N-mm)
M_{max}	Maximum potential flexural resistance, kip-in (N-mm)
M_y	Yield moment, $F_yS_x = F_yS_{xc} = F_yS_{xt}$, doubly-symmetric sections and channels bent about major axis; smaller of M_{yc} and M_{yt}, singly-symmetric sections bent about major axis, kip-in (N-mm)
M_{yr}	Yield moment capacity considering compression flange residual stress effects, $F_{yr}S_{xc}$, kip-in (N-mm)(?)
R_h	Hybrid girder factor
S_x	Elastic section modulus, doubly-symmetric sections and channels bent about major axis, in^3 (mm^3)
S_{xc}	Elastic section modulus corresponding to the extreme compression fiber, in^3 (mm^3)
X^2	Ratio of the bending to the torsional efficiency of the cross-section, specified by Eq. (7b)
X_1	Beam buckling factor defined by AISC LRFD Specification (AISC 1999) Equation F1-8
X_2	Beam buckling factor defined by AISC LRFD Specification (AISC 1999) Equation F1-9
b_f	Flange width, doubly-symmetric I-shapes and channels, in (mm)
b_{fc}	Width of a rectangular compression flange, in (mm)
b_{ft}	Width of a rectangular tension flange, in (mm)
c	Section factor associated with the elastic lateral-torsional buckling resistance of channels
d	Total depth between the extreme fibers of the flange elements perpendicular to the major axis of bending, in (mm)
h	Distance between the centroids of the flange elements perpendicular to the major axis of bending, in (mm)
m	A multiple of the yield strength corresponding to the compression flange state within a heavily plastified cross-section
r_E	Equivalent column radius of gyration corresponding to elastic lateral-torsional buckling strength, in (mm)
r_t	Radius of gyration for lateral-torsional buckling defined by Eq. (7a) for doubly-symmetric I-shapes and channels and by Eq. (13) for doubly- or singly-symmetric I-shapes with rectangular flanges, in (mm)
r_y	Radius of gyration about y axis, in (mm)
r_{yc}	Radius of gyration of the compression flange taken about the y axis, in (mm)
t_f	Flange thickness, doubly-symmetric I-shapes and channels, in (mm)
t_{fc}	Compression flange thickness, in (mm)
t_{ft}	Tension flange thickness, in (mm)
t_w	Web thickness, in (mm)
v	Poisson's ratio of steel, 0.3